GAS ENTROPY IN NEARBY GALAXY CLUSTERS

G.W. Pratt[1], M. Arnaud[2], and E. Pointecouteau[3]

[1]MPE Garching, Giessenbachstraße, Garching, Germany
[2]CEA/Saclay Service d'Astrophysique, L'Orme des Merisiers, Bât. 709, 91191 Gif-sur-Yvette Cedex, France
[3]CEA/Saclay Service d'Astrophysique & Astrophysics, University of Oxford, Keble Road, Oxford OX1 3RH, UK

ABSTRACT

We investigate the scaling properties of the ICM entropy using *XMM-Newton* observations of a sample of ten nearby ($z < 0.2$) galaxy clusters covering a decade in mass ($\sim 10^{14} - 10^{15}\,M_{\odot}$). We examine the scaling properties of the entropy with system temperature, and explore the structural properties of the scaled entropy profiles. We discuss our results in the context of the effect of non-gravitational processes on observed cluster X-ray properties.

Key words: Cosmology: observations, Galaxies: cluster: general, (Galaxies) Intergalactic medium, X-rays: galaxies: clusters.

1. INTRODUCTION

Observations of the entropy of the hot, X-ray emitting intracluster medium (ICM) of galaxy clusters are fundamental for understanding the thermodynamic history of the gas. Entropy is generated in shocks as the gas is drawn into the potential well of the cluster halo, thus the quantity reflects the accretion history of the ICM. However, the entropy distribution also preserves key information regarding the influence and effect of non-gravitation processes on the properties of the ICM.

Observations with *ROSAT* and *ASCA* indicated an excess in entropy in the coolest systems at $0.1R_{200}$ (hereafter $S_{0.1}$). The entropy at that radius is considerably higher than that available from gravitational collapse (Ponman et al., 1999; Lloyd-Davies et al., 2000), leading to a shallower entropy-temperature (S–T) relation than expected. More recent spatially resolved entropy profiles indicate that the entropy is higher *throughout* the ICM, and that, outside the core regions, entropy profiles are structurally similar (Ponman et al., 2003; Voit & Ponman, 2003; Pratt & Arnaud, 2003, 2005; Piffareti et al., 2005). At the same time the scatter in $S_{0.1}$ at a given temperature can be up to a factor of three (Ponman et al., 2003).

Preheating, where the gas has been heated before being accreted into the potential well, by early supernovae and/or AGN activity (e.g., Kaiser, 1991; Evrard & Henry, 1991; Valageas & Silk, 1999), internal heating after accretion (e.g., Metzler & Evrard, 1994), and cooling (e.g., Pearce et al., 2000) can all have different effects on the structure and scaling of the entropy in clusters. The lack of isentropic core entropy profiles in groups and poor clusters has shown that simple preheating is unlikely to be the sole explanation of the observations (Ponman et al., 2003; Pratt & Arnaud, 2003, 2005). Since cooling-only models generally predict a higher stellar mass fraction than observed (e.g., Muanwong et al., 2002), attention is now focussing on the interplay between cooling and feedback. Further high quality observations are needed in order to distinguish between these different entropy modification mechanisms.

Here we present a summary of results from *XMM-Newton* observations of ten nearby morphologically relaxed systems: A1983 (z = 0.0442), A2717 (z = 0.0498), MKW9 (z = 0.0382), A1991 (z = 0.0586), A2597 (z = 0.0852), A1068 (z = 0.1375), A1413 (z = 0.1427), A478 (z = 0.0881), PKS0745-191 (z = 0.102) and A2204 (z = 0.1523). Full results can be found in Pratt et al. (2006) (astro-ph/0508234).

2. RESULTS

2.1. Entropy scaling

In Fig 1, the entropy profiles are shown plotted in terms of the measured virial radius, R_{200} (see Pointecouteau et al. 2005 for details). All profiles increase monotonically with radius and, while the slope of the profile becomes shallower towards the centre in some of the clusters, none shows an isentropic core.

Estimating the entropy at various fractions (0.1, 0.2, 0.3 and 0.5) of the virial radius, we plot in Figure 2 the relation between entropy and global temperature. A power-law fit to the data at each radius yields the results shown

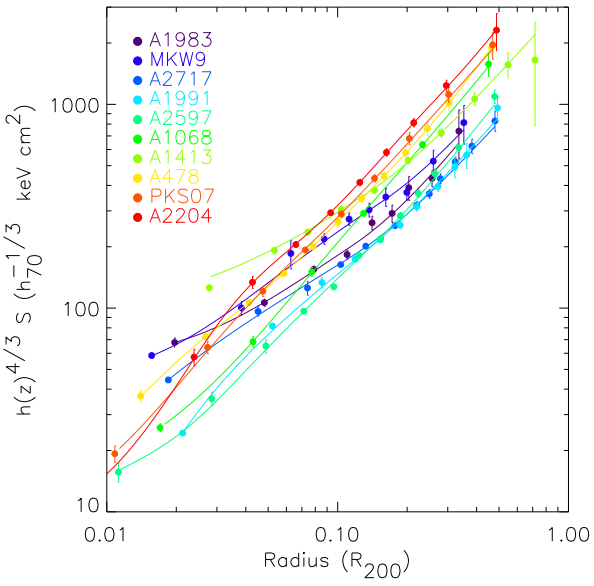

Figure 1. *Cluster entropy profiles obtained from the deprojected, PSF corrected temperature profiles and the best fitting analytical model for the gas density. Solid lines, included to improve visibility, are entropy profiles obtained from analytic model fits to the temperature and density information.*

Table 1. *The S–T relation. Data were fitted with a power-law of the form* $h(z)^{4/3}\ S = A\times(kT/5\mathrm{keV})^{\alpha}$, *where* kT *is the overall spectroscopic temperature in the* $0.1-0.5\ R_{200}$ *region. Errors in entropy and temperature are taken into account. Results are given BCES regression method (see text). Statistical and intrinsic scatter about the best fitting relation in the log-log plane are given in the last columns.*

Radius	A	α	σ_{log}	
R_{200}	keV cm^{-2}		stat	int
BCES				
0.1	230 ± 17	0.49 ± 0.15	0.082	0.076
0.2	485 ± 22	0.62 ± 0.11	0.063	0.052
0.3	798 ± 44	0.64 ± 0.11	0.078	0.065
0.5	1560 ± 83	0.62 ± 0.08	0.074	-

in Table 1. The slope of the entropy-temperature relation is incompatible with the standard self-similar prediction at all radii at which we have measured it, confirming the results of Ponman et al. (2003). The slope of the $S_{0.3}$-T relation, obtained using the BCES method, is $S_{0.3} \propto T^{0.64\pm0.11}$, in excellent agreement with that found by Ponman et al. (2003). Figure 2 shows that there is noticeable scatter about the S–T relation at $0.1\,R_{200}$. Table 1 makes clear that the scatter is reduced at larger scaled radius. The intrinsic scatter remains the dominant contributor to the dispersion in all relations, except at $0.5\,R_{200}$.

2.2. Entropy structure

In Fig. 3 we show the profiles scaled using the relation $S \propto h(z)^{-4/3}\,T_{10}^{0.65}$, where T_{10} is the global temperature measured in units of 10 keV. This relation is consistent

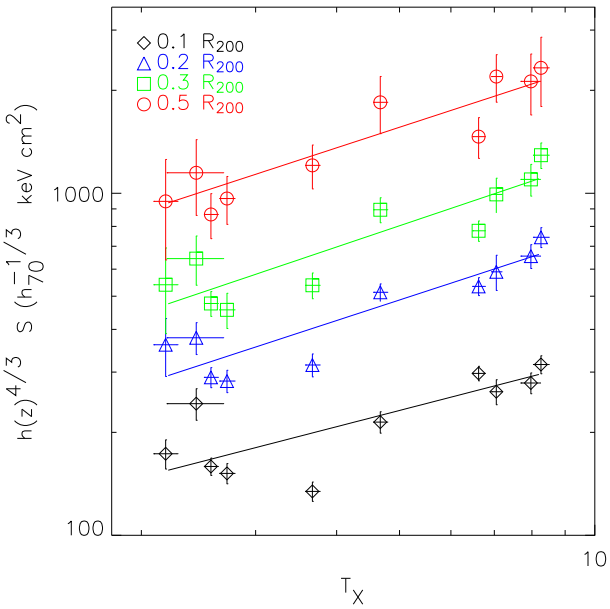

Figure 2. *The S-T relation measured from a sample of 10 clusters covering a temperature range from 2 to 9 keV. The S-T relation is shown for different fractions of* R_{200}. *Measurements are plotted with error bars. At each radius, the best-fitting power-law relation, derived taking account the errors in entropy and temperature, is overplotted; slopes and intercepts are given in Table 1.*

with our data (Table 1), and allows us to compare our results with previous work. As an initial measure of the scatter in scaled entropy profiles, we estimated the dispersion at various radii in the range 0.02–$0.45\,R_{200}$. The shaded area in Fig 3 shows the region enclosed by the mean plus/minus the 1σ standard deviation. Figure 3 shows that, outside the core regions, the entropy profiles present a high degree of self-similarity. The relative dispersion in scaled profiles remains approximately constant at $\lesssim 20$ per cent for $r \gtrsim 0.1\,R_{200}$, in excellent agreement with the dispersion found in a smaller subsample by Pratt & Arnaud (2005). In the core regions, however, the dispersion increases with decreasing radius to reach $\gtrsim 60$ per cent at $\sim 0.02\,R_{200}$.

Fitting the scaled profiles with a power law using the BCES method in the radial range $r \geq 0.01\,R_{200}$ we find a slope of 1.08 ± 0.04, with a dispersion of ~ 30 per cent about the best fitting line. The slope is not significantly changed (1.14 ± 0.06) if the data are fitted in the radial range $r \geq 0.1\,R_{200}$, but the intrinsic dispersion is two times smaller (14 per cent).

3. DISCUSSION

Our results put into evidence two main departures from the standard self-similar model of cluster formation. First, beyond the core region ($r \gtrsim 0.1\,R_{200}$) the entropy profiles obey self-similarity, having a shape consistent with expectations, but with a modified temperature (or

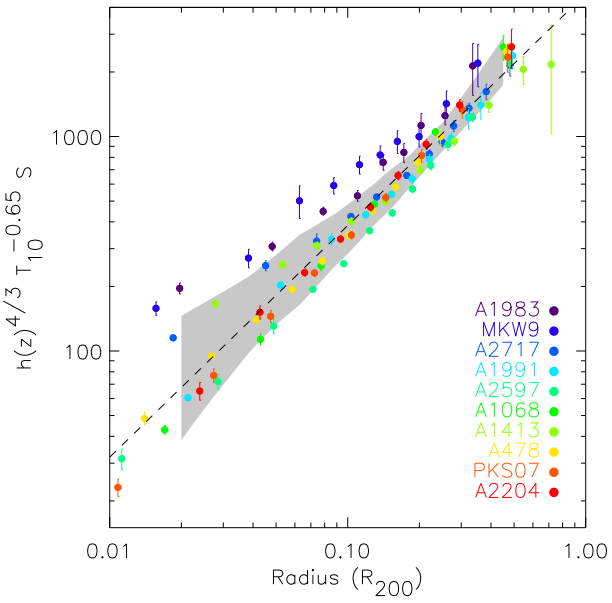

Figure 3. *Scaled entropy profiles. The radius is scaled to R_{200} measured from the best-fitting mass models. The entropy is scaled using the empirical entropy scaling $S \propto h(z)^{-4/3} T_{10}^{0.65}$, using the global temperature in units of 10 keV. The shaded grey area corresponds to the region enclosed by the mean plus/minus the 1σ standard deviation. The dashed line denotes $S \propto R^{1.08}$.*

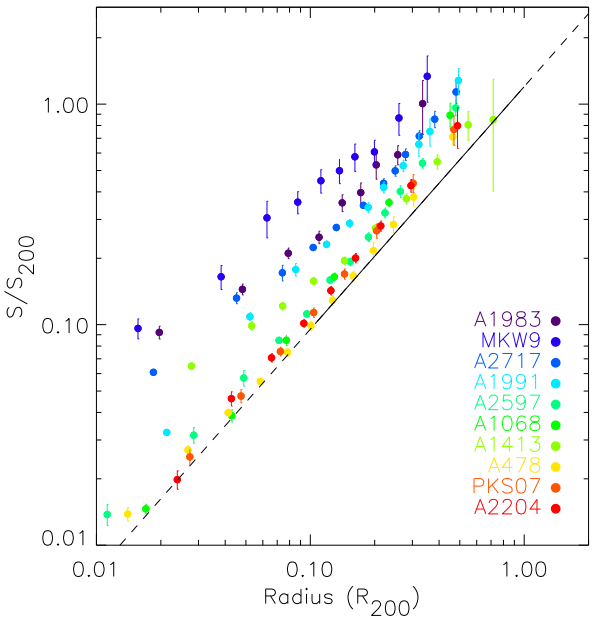

Figure 4. *A comparison of our observed entropy profiles with the prediction from the adiabatic numerical simulations of Voit (2005). The observed entropy profiles have been scaled to S_{200} using Equation 1. The solid line represents the best-fitting power law relation found by Voit (2005) from fitting adiabatic numerical simulations of 30 clusters in the radial range $0.1 < R_{200} < 1.0$.*

mass) scaling. The scaling relations are shallower than expected. Second, there is a break of similarity in the core region: the dispersion in scaled profiles increases with decreasing radius.

3.1. Entropy normalisation

The modified entropy scaling indicates that there is an excess of entropy in low mass objects *relative* to more massive systems, as compared to the expectation from pure shock heating. A comparison with adiabatic numerical simulations allows us to quantify the *absolute* value of the excess and to examine whether an entropy excess is also present for the most massive systems. Voit (2005) shows the results of adiabatic numerical simulations of 30 clusters spanning a mass range of more than a factor of ten. Once scaled by the characteristic entropy of the halo S_{200}, the simulated profiles are closely self-similar, and can be well fitted in the radial range $\sim 0.1 - 1.0\ R_{200}$ by the power-law relation $S/S_{200} = 1.26(R/R_{200})^{1.1}$. Assuming $f_b = 0.14$ ($\Omega_b h^2 = 0.02$ and $\Omega_m = 0.3$) and typical elemental abundances, we can scale our observed entropy values to S_{200} using the expression

$$S/S_{200} = \left(\frac{S}{2471\ \mathrm{keVcm}^2}\right)\left(\frac{M_{200}}{1 \times 15 M_\odot}\right)^{-2/3} h(z)^{2/3}. \quad (1)$$

Further scaling the radius by the measured value of R_{200} allows us to compare our results directly with the adiabatic simulations. In Figure 4, our observed entropy profiles are compared with the prediction of Voit (2005).

The richer systems all have entropies which are in good agreement (both in slope and normalisation) with the adiabatic prediction, denoted by the solid line in Fig. 4. On average, their entropy is only slightly higher than predicted (by $\sim$ 20 per cent), although the effect is not very significant. We recall that there is also a $\sim$ 30 per cent difference in normalisation between the observed M–T relation and that predicted by adiabatic simulations (Arnaud et al., 2005). Interestingly, this corresponds to a $\sim$ 20 per cent entropy excess at a given mass for $T \propto M^{2/3}$. The (slight) excess of entropy in massive systems is thus consistent with a simple increase of the mean temperature, i.e., of the internal energy of the ICM. However, Fig. 4 shows explicitly that the poorer systems have a systematically higher entropy normalisation than the richer systems. There is approximately 2.5 times more entropy at $0.2\,R_{200}$ in the ICM of A1983, the poorest cluster in our sample, than that predicted by gravitational heating. This excess shows that the density of the ICM is also affected at lower mass.

Voit et al. (2003) and Ponman et al. (2003) independently noted that the ICM entropy is highly sensitive to the density of the incoming gas and suggested that a smoothing of the gas density due to pre-heating in filaments and/or infalling groups would boost the entropy production at the accretion shock. Recent numerical simulations which mimic preheating by imposing a minimum entropy floor at high z have confirmed the entropy amplification effect

due to smooth accretion (Borgani et al., 2005). However, the effect seems to be substantially reduced when cooling is also taken into account. Furthermore, the physical origin of the preheating is still unclear.

3.2. Localised modification

The adiabatic numerical simulations of Voit (2005) show both a flattening of the slope and an increase in the dispersion of the scaled entropy profiles in the central regions ($< 0.1\ R_{200}$). However, the dispersion in our observed profiles (~ 60 per cent) greatly exceeds that of the simulations (~ 30 per cent, cf Fig. 4 and Fig. 11 of Voit 2005). Six clusters out of our total sample of ten (A1991, A2597, A1068, A478, PKS0745 and A2204) have remarkably similar scaled entropy profiles, displaying power-law behaviour down to the smallest radii measured. These six clusters all appear to host a bona fide cooling core, each having a central temperature decrement of a factor ~ 2. Strong radiative cooling thus appears to generate entropy profiles which display power-law behaviour down to very small radii (Fig. 4).

The other four clusters in our sample are characterised by a smaller central temperature decrement, larger cooling times and shallower entropy profiles. Clearly, some mechanism has modified the cooling history of these clusters. Energy input from AGN is regularly invoked as a way of moderating cooling at the centres of galaxy clusters. Our sample contains four clusters which have X-ray evidence for interactions between radio and X-ray plasma (A478, A2204, A2597, and PKS0745), and yet the entropy profiles of all of these clusters increase monotonically outward in the canonical fashion. It is possible that the heating is distributed via e.g., weak shocks (Fabian et al., 2003), thus preserving the generally increasing form of the entropy profile.

Merging events can result in substantial mixing of high and low entropy gas. Such redistribution of entropy will depend on the scale of the merger, whether the merger has disrupted the structure of the cool core, and the timescale for re-establishment of the cool core if disrupted. In the current sample MKW9, A2717, A1413 and A1983 all have flatter core entropy profiles. We note that the morphological information for the present sample would argue against recent merger activity in these clusters (Pratt & Arnaud 2005; Arnaud et al. 2005; Pointecouteau et al. 2005). However, this does not rule out entropy modification due to a more ancient merger, particularly if the relaxation time is less than the cooling time.

These will be interesting questions to address with numerical simulations. On the observational side, comparison with a larger, unbiased, sample of clusters is ongoing.

ACKNOWLEDGMENTS

GWP thanks E. Belsole and J.P. Henry for useful discussions, and acknowledges funding from a Marie Curie Intra-European Fellowship under the FP6 programme (Contract No. MEIF-CT-2003-500915). EP acknowledges the financial support of CNES, the French Space Agency, and of the Leverhulme trust (UK).

REFERENCES

Arnaud, M., Pointecouteau, E., Pratt, G.W., 2005, A&A, 441, 893

Borgani, S., Finoguenov, A., Kay, S.T., Ponman, T.J., Springel, V., Tozzi, P., Voit, G.M., 2005, MNRAS, 361, 233

Evrard A.E., Henry J.P, 1991, ApJ, 383, 95

Fabian, A.C., Sanders, J.S., Allen, S.W., Crawford, C.S., Iwasawa, K., Johnstone, R.M., Schmidt, R.W., Taylor, G.B., 2003, MNRAS, 344, L43

Kaiser, N. 1991, ApJ, 383, 104

Lloyd-Davies E.J., Ponman, T.J., Cannon, D.B., 2000, MNRAS, 315, 689

Metzler, C.A., Evrard, A.E., 1994, ApJ, 437, 564

Muanwong, O., Thomas, P.A., Kay, S.T., & Pearce, F.R. 2002, MNRAS, 336, 527

Pearce, F.R., Thomas, P.A., Couchman, H.M.P., Edge, A.C., 2000, MNRAS, 317, 1029

Piffaretti, R., Jetzer, P., Kaastra, J.S., Tamura, T., 2005, A&A, 433, 101

Pointecouteau, E., Arnaud, M., Pratt, G.W., 2005, A&A, 435, 1

Ponman, T.J., Cannon, D.B., Navarro, J.F., 1999, Nature, 397, 135

Ponman, T.J., Sanderson, A.J.R., Finoguenov, A., 2003, MNRAS, 343, 331

Pratt, G.W., Arnaud, M., 2003, A&A, 408, 1

Pratt, G.W., Arnaud, M., 2005, A&A, 429, 791

Pratt, G.W., Arnaud, M., & Pointecouteau, E. 2006, A&A, in press (astro-ph/0508234)

Valageas, P., & Silk, J. 1999, A&A 347,1

Voit, G.M., Balogh, M.L., Bower, R.G., Lacey, C.G., Bryan, G.L., 2003, ApJ, 593, 272

Voit, G.M., Ponman, T.J., 2003, ApJ, 594, L75

Voit, G.M. 2005, Rev. Mod. Phys., 77, 207